S-Wave Velocity Structure beneath Southwest North America from Seismogram Comparisons of the Mexico Earthquake on 22 June 1997

Bagus Jaya Santosa

Prodi Geofisika, Fisika, FMIPA, ITS,
Jl Arif Rahman Hakim 1, Kampus ITS Sukolilo,
Surabaya 60111, Indonesia
Email: bjs@physics.its.ac.id

Abstract. This research investigates earth structure beneath the Southwest North America landmass, especially between Mexico and California. Models based on S wave velocities for this area were obtained by carrying out seismogram fitting in time domain and three Cartesian components simultaneously. The data used is from an event, coded as C052297B that occurred in the state of Guerrero, Mexico and it was fitted to synthetic data computed with the GEMINI program at TS network stations. Earth model IASPEI91 and SPREM were used as input to create the synthetic data. Real and synthetic seismograms were subjected to a low-pass filter with a frequency corner of 20 mHz.

Waveform analysis results show very unsystematic and strong deviations in the waveform, arrival times, amount of oscillation and the height of the wave amplitude. Discrepancies are met on S, Love, Rayleigh and ScS waves, where the stations epicentral distances are below 30^0. Deviation in analysis waveform because of the usage of model 1-D of SPREM and IASPEI91, because the 1-D was a kind of average value an elastic property at one particular depth of global earth. With the method of waveform analysis we can see how sensitive waveform is to structures within the layers of the Earth.

To explain the discrepancies, a correction to the earth structure is essential. The corrections account for the thickness of the crust, speed gradient of β_h, the coefficient for the β_h and β_v in the upper mantle for surface wave fitting, a small variation of the S speed structure at a layer under the upper mantle above 771 km for S wave fitting, and a small variation at the base the mantle layers for ScS wave fitting. At some stations, a correction for S speed structure have yielded P wave fitting.

Results of this research indicate that the 1-D earth model obtained through seismogram fitting at every hypocenter-observation station pair is unique. The S-wave velocity on the upper mantle has strong negative anomalies. This paper criticized the previous earth models in the same area, which have been published by other seismologists, by analyzing the seismogram of C052297B earthquake in the TS seismological network station

Received February 28th, 2007, Revised October 27th, 2007, Accepted for publication December 12th, 2007.

Keywords: *differently S speed structure upper mantle – CMB; seismogram fitting; strong negative anomaly under South West North America.*

1 Introduction

On May 22, 1997 an earthquake with moment magnitude (Mw) 6.5 occurred in Guerrero, Mexico, coded as C052297B. Such moderate earthquake put already into vibration the whole content of the Earth and as a result sensitive equipment on the surface of the planet can measure them. Ground movement is measured using a seismometer at a receiver station. A signal in the form of displacement, velocity or acceleration [mm, mm/s or mm/s^2] becomes Voltage (mV), and eventually is recorded as time series data. The data can be represented as a seismogram, which consists of complex wave phases that occur as a result of reflections and refractions within the body of the Earth. This shows the existence of a difference in the elastic parameter of the layers on an Earth model. Wave propagation from the earthquake source to the station overcomes various interfaces, which results in overlapped wave phases on the seismogram.

Analyzing quantitatively the seismogram is to measure the arrival time of especial wave phase, arrival time difference, and polarity of the P wave, the S/P ratio amplitude, and the relation between phase/group speeds by period/frequency at surface waves, the so-called dispersion analysis. The easiest arrival time to note is the onset of the P wave. The arrival time of subsequent phases, such as the S wave is not so easy to measure, because the frequency content becomes lower and the wave phase overlaps.

The travel time of certain wave phases can be used by seismologist to derive Earth models, like SPREM [1], IASPEI91 [2] and AK135 [3]. These models, either global or regional, can tell us something about the earthquake source, either the hypocenter or origin time of the earthquake and the earthquake mechanism.

Using one of these models the travel time of various wave phases between hypocenter and station can be computed. This arrival time is used as a guide to identify the wave phase in seismograms. Using a time curve and the time difference between some main phases, the epicentral distance can be determined. Using data of observation stations that are around the epicenter, the location of the earthquake epicenter can be determined [4, Ch. 4].

Data obtained by the hypocenter-station pair and the various wave phases from thousands of earthquakes during tens of years can reach the amount of millions of data points. Earth models, like IASPEI91 and SPREM benefit from having better resolution by the addition of more data. As opposed to the P wave travel time data, the S wave data is scarce [1]. Elastic parameters are obtained through travel time method of P and S wave velocities. Correctness of P wave speed structure is better than structure of those based on S waves, because the record keeping of S wave arrival times are more difficult due to the lower frequencies of S wave. Other elastic parameters, such as mass density, quality factor of damping and anisotropy are obtained by using methods of dispersion analysis of surface wave.

There are various method of computing travel times [5-7] that can be applied to obtain the structure of P and S wave velocities in 1, 2 or 3-D Earth model, whose earth structure and heterogeneity in the mantle, and the structures of S speed near the CMB and core are analyzed through the travel time of SKKS waves. Such wave phase can be observed at station with epicentral distances greater than 83^0 [8, 9].

Tomography is a dispersion analysis method, where observed data measures the relation between phase/group velocities to frequencies/periods. There are various methods to measure the dispersion curve, for example Multiple Filtering Technique [10], which matches the phases for the insulation of basal mode of surface wave [11]. Inversion is carried out with the goals to get the fitting between observed and predicted group velocities. From this fitting, a more detail 1-D or 3-D model of the Earth can be obtained [12-15].

Both methods to obtain the earth models are obtained by evaluating only a little information of the seismogram. This research analyzes the waveform in the time domain with three components simultaneously, where the all relied information in the seismogram is analyzed. It will be shown how sensitive a waveform is to structure of an Earth model by covering structures of speed and anisotropy within the Earth. This research also shows at what depth the layers meet the vertical isotropy in the Earth model. The standard Earth model that is often raised as a reference by all experts in seismology is IASPEI91 and SPREM (but we used the anisotropic version of SPREM, so called as PREMAN) is shown in Figure 1.

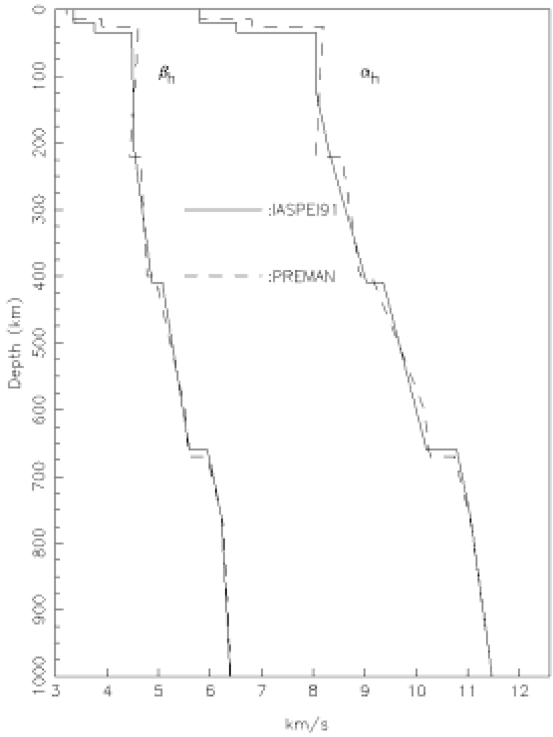

Figure 1 Standard Earth models: The isotropic IASPEI91 and the vertical anisotropic SPREM (PREMAN) up to 1000 km depth.

This study tries to answer the following question: Although the seismogram analysis is carried out with a corner frequency of 20 mHz, are standard earth models obtained by evaluating a small amount of information on a seismogram and yet return a synthetic seismogram with three components similar to the observed one?

We approach the method of exploiting the overall information on the seismogram in the time domain and the three Cartesian components simultaneously. This method differs from other tomography methods carried out in the same area (Central America, [12]), which have been done based on the analysis of P and S wave arrival times [16] and the dispersion analysis, which are specifically done at vertical component of Rayleigh [14, 17] and Love waves separately [18]. This paper criticized the earth models in the same area (Central America), which have been published by other seismologists. The used data is the seismogram of C052297B earthquake in the TS (TERRAScope) seismological network station.

The method of simultaneously analyzing the seismogram in time domain with three components is the best approach [4]. On the contrary the other seismologists use the data, where they were evaluated only at some points in the seismogram (travel time and dispersion data). The synthetic seismogram is computed with the GEMINI program [19, 20], where the input is a completely elastic Earth model, hypocenter depth, the CMT solution of an event C052297B, and the location of the observing stations. In order to compare the synthetic and real seismogram in the same units, the file response from the observation station was used. Seismogram data was downloaded from the Incorporated Research Institutions for Seismology website (IRIS, http://www.iris.edu).

2 Research methodology

Every earthquake yields ground movement any station can record its three Cartesian component (N-S, E-W and vertical Z) known as channels with the suffix – E – N & -- Z. The location of the earthquake epicenter is in Guerrero, Mexico, with coordinates 18.68^0 North Latitude and 101.60^0 West Longitude and 55.5 km depth. To dissociate the component of the ground movement in direction of transversal and radial movements, the horizontal area formed by the orientation of the local N-S and E-W at the observation station have to be rotated, in such a way that the rotating angle is between the local 'North' and the direction of a small arc from the station to the epicenter (back-azimuth). Rotation on the horizontal plane is needed to dissociate the movement due to the wave propagation mode of P-SV and SH wave.

To obtain the synthetic wave phases, program TTIMES is used to compute the travel times calculations. Program TTIMES is based on the article from Buland and Chapman [21], which can be obtained from http://orfeus.knmi.nl.

The calculation of synthetic seismogram is based on the GEMINI method [19, 20]. This method is equivalent to the method of Mode Summation, except the free variable is complex frequency not the real frequency only, but the corner frequency can be set to an arbitrary frequency. When running the program, an Earth model, either IASPEI91 or SPREM is given as input. The elastic parameters of the model contains data that describes the structure, density, quality factor, μ and κ, which are essential for computing the propagation of the compression and shear waves.

GEMINI, stands for Green's function of the Earth by MINor Integration, is a program to calculate the minors of the Green functions for an earth model and for a certain depth of earthquake source. The green's functions are expanded (integrated) by fulfilling the physical conditions in the returning point of wave (the deepest point in wave propagation), the depth point of source and the border conditions in the earth surface. The expansion is written using the independent variable as a complex frequency by inserting a trick damping (ω + $i\sigma$) to avoid time aliasing. The earthquake tensor moment detailed in the third line of the CMT (Centroid Moment Tensor) solution was used to calculate the coefficients of Green's function through the accomplishment of the Cramer rule on the Green's function. The right side of linear equations is the coefficient series of the tensor moments. The coordinate of earthquake source was put as the North Pole, and the coordinate of the observation station was changed into a form of epicentral and azimuth angle. The spherical harmonic function was developed with these two angle values. The DISPEC program (belongs to Gemini Package) reads the Green's function that has been outputted by GEMINI program and forms a multiplication with the coefficients of expansion on the Moment Tensor and the spherical harmonic function and then sums them, resulting the synthetic seismogram in the complex frequency domain. The GEMINI package has taken into account the earth model, focal mechanism and moment of the earthquake. The MONPR program (GEMINI Package) transforms the synthetic seismogram from the complex frequency domain into the time domain. The measured and synthetic seismograms were subjected to a Butterworth low-pass filter. The inverse RESPONSE file from the seismometer equipment system on the receiver station was imposed to the measured seismogram, i.e. the description about the phase change and the amplification of the equipment system while changing the input of the land-movement in velocity/acceleration into the output Voltage. The horizontal component of the measured seismogram should be rotated with the X axis (East-West canal) was directed to the small arch formed by the observation station of the earthquake source (back-azimuth), refer to Figure 1. The purpose was to decompose the wave movement in 3-D space into the components of P-SV and SH. Therefore the synthetic and measured seismograms were compared in the same unit and movement direction.

Elastic parameters in the IASPEI91 earth model are not as complete as those contained in the SPREM earth model. Therefore, the elastic parameters, which are not owned by the IASPEI91, are loaned from SPREM model.

The amount of data in the time domain seismogram comparison with three components is on the order of thousands, hence, a change made on the crust, the speed of the gradient, and the zeroed order coefficient value in the speed polynomial are conducted through a trial and error method.

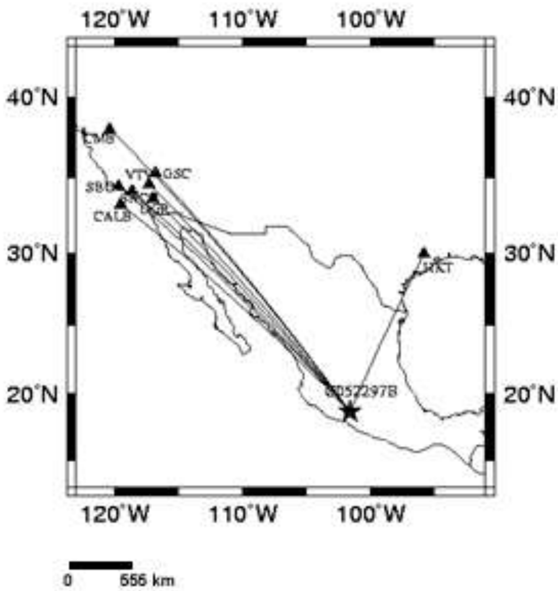

Figure 2 Ray paths from epicenter to stations CALB, CMB, DGR, SBC, VTV and SNCC.

3 Results and Analysis

This study analyzed the seismic data from the May 22, 1997 Guerrero, Mexico earthquake at stations CALB, CMB, DGR, SBC, SNCC and VTV (Figure 2).

Figure 3 shows a comparison between observed and synthetic seismograms. The figure lower portion shows a seismogram comparison between the synthetically computed seismogram, computed with SPREM, and the upper set is from IASPEI91 earth model. To identify the wave in seismogram, the travel time of some wave phases is used, which is calculated by TTIMES program from IASPEI91 earth model (expressed as vertical lines in the figure). A set of picture consists of three traces; the lowest trace shows the vertical movement in z component, the middle is for radial component and uppers is for transverse component. The abscissa axes is the time after the Origin Time, the tick marks distance is in minutes, while ordinate axes is to express the amplitude comparison.

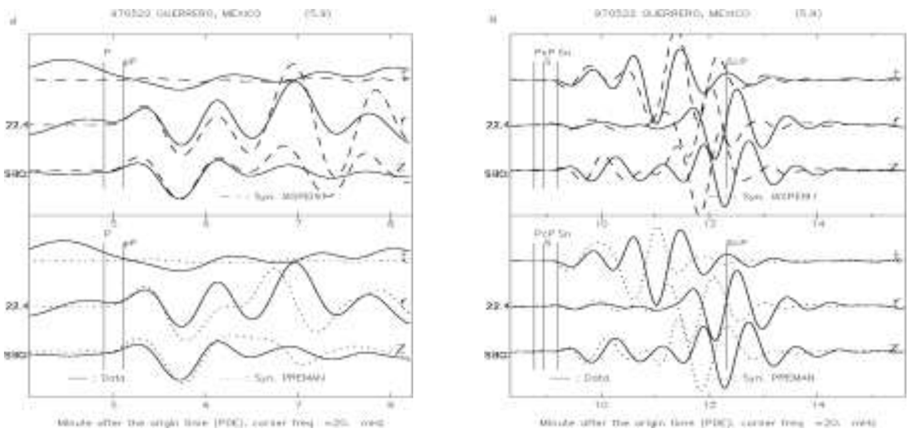

(a) (b)

Figure 3 Seismogram comparison in observation station SBC between data and synthetics that are from SPREM and IASPEI91. Time window: (a) P wave; (b). S, L and R Wave.

It will be shown, how is the seismogram analysis if carried out with the corner frequency of low-pass filter set at 20 mHz. Seismogram Data is property of station SBC, where the station's epicentral distance is 22.4^0. Figure 3 presents seismogram comparison between data and synthetics, where lower picture set is formed from SPREM and upper is IASPEI91 earth model. Figure 3a shows seismogram comparison between data and synthetics at time window of P wave. It can be seen, that a P waveform from IASPEI91 arrives 8 seconds early than the real P waveform, but the synthetic P repetitive waveform that arrives on 7 minute, has bigger amplitude than the real P repetitive. Meanwhile that synthetic P waveform from SPREM shows 4 s early arrival time than the real P, while the synthetic from SPREM in 7 minute arrives much early. There is no notation for this wave phase, is not given by program TTIMES, but this phase is clearly not the PPP wave, because due small epicentral distance, the arrival time this PPP phase arrives not far from PnPn wave arrival. This is also not from the earth core reflected PcP wave, because the arrival time starts to come in 8'46". Thereby, GEMINI method used to calculate the synthetic seismogram give the complete seismogram for all wave phases. Figure 3b shows seismogram analysis at time window of S wave until the surface wave. Seismogram analysis on the synthetic seismogram from SPREM in z component shows that this synthetic arrives earlier than the real S, while the synthetic S from IASPEI91 arrives much earlier. For a while on t component the synthetic S from SPREM shows a relative good arrival time, whereas synthetic SH phase from IASPEI91 arrives earlier than real SH. Further analysis is done on Love surface wave. It can be seen, that waveform from synthetic Love from SPREM approaches well the real Love waveform, but the synthetic Love arrives earlier than the real

Love, while waveform from IASPEI91 gives a bigger amplitude and longer oscillation. Perception is by the waveform comparison at Rayleigh wave, it shows that the synthetic from both standard earth models deviates far away from the real Rayleigh wave. The arrival time of the main oscillation disagrees with the real data till 27 second. This is big enough, because epicentral distance is only 22.4^0 and this is also bigger than the other arrival time difference.

After observing some deviations that met by seismogram comparison above, research problem has aim to achieve the fitting at surface wave, because this wave propagates on shallower earth layers, that is covering the arrival time and oscillation amount at Love wave and arrival time of Rayleigh wave. Surface wave propagates long as the earth surface tills a depth which its deepness is equivalent to the surface wavelength [22]. Therefore the speed structure in upper mantle will be altered, in such a way till the fitting between seismogram observation and synthetic is achieved. Besides, it will be seen whether corrective result at structure of S wave velocity at deeper layers will give the fitting at S wave. It will further be investigated, whether the structure of S-wave velocity will give the contribution for the repair at P wave, it will be shown at following analysis.

The earth model IASPEI91 is formed only from travel time data so that elastic parameters yielded are only speed of P and S wave. It is a surprise, that earth model IASPEI91 can give the better fitting than SPREM model on Love wave, whether this effect comes only due to difference in earth crust thickness. Beside that the earth model IASPEI91 is in the form of isotropic earth, though seismogram comparison at surface wave explains self, that anisotropic earth model shall to be used to execute the inversion of both surface wave simultaneously. Therefore further seismogram comparison are relied on seismogram synthetic yielded from an anisotropic earth model SPREM and corrected earth model.

Speed correction is done at upper mantle layers, where changes cover the usage of positive gradient for the β_h and zero order coefficient of polynomial speed function for the β_h and β_v in upper mantle layer, while speed gradient for the β_v let like initially as SPREM model. Result from this correction can be seen at Figure 4a for the time segment of P wave, where synthetic P from the corrected earth model has the arrival time which is equal as real P, as well as waveform of P repetitive that can be good simulated. Nevertheless is the real wave phase which arrives at the minute 7'48", is still difficult to simulate, because correction is only done on S-wave velocities only. This is the topic for other seismologist to explain this P repetitive wave.

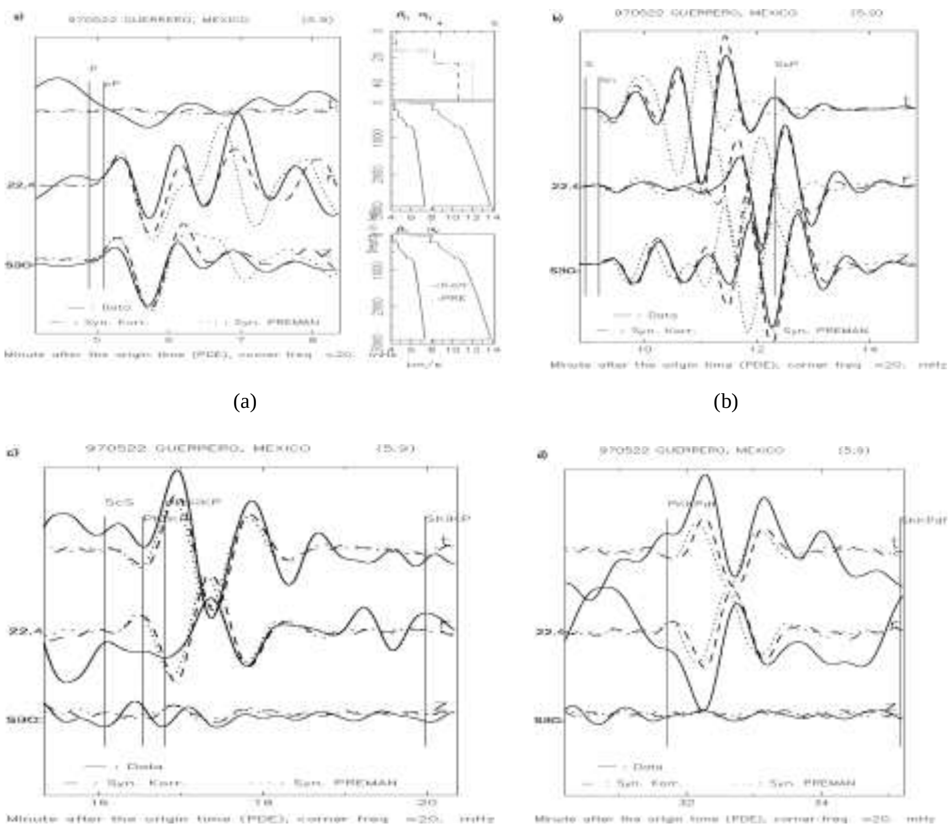

(a) (b)

(c) (d)

Figure 4 Seismogram fitting in observation station SBC in time window of: (a) P; (b) S, L and R; (c) ScS; (d) ScS_2 wave.

Figure 4b shows seismogram comparison at time window of S wave till Rayleigh wave. It is interesting that fitting at all of wave phase is achieved, starting from wave S, and Love wave till Rayleigh wave and at three Cartesian components simultaneously. Fitting to the Rayleigh wave at z and r components are done only by altering the zero order coefficients of speed polynomial function, the β_v in upper mantle, while for the Love wave the corrections cover the gradient and zero order coefficients. To correct the S wave is a speed change on layers till 771 km depth, where the order of corrections is very small, below 0.5%. But corrections for the β_h and β_v requires the differently values, because the delay of synthetic SV and SH is differ. This indicates that the anisotropy is also met on layers below the upper mantle till 771 km. Figure 4c and 4d show seismogram analysis seismogram on ScS and ScS_2 wave. It can be seen that synthetic ScS waveform from corrected earth model fits well the real ScS waveform. To achieve this fitting is a speed correction β_v and β_h till CMB also conducted. Corrections on β_v and β_h in upper 771 km give small repair on depth waves. Therefore corrections are continued on S wave velocity in the base mantle. Waveform analysis on the ScS waveform at epicentral distance as so small as this, gives new road to investigate the structure of S speed from CMB till upper mantle. The ScS and ScS_2 waveform analysis gives the better method compared to method of differential travel time of SKKS and S-SKKS wave, where with this method is the speed structure in the near of CMB investigated, that needs the observation stations with big epicentral distance [8, 9].

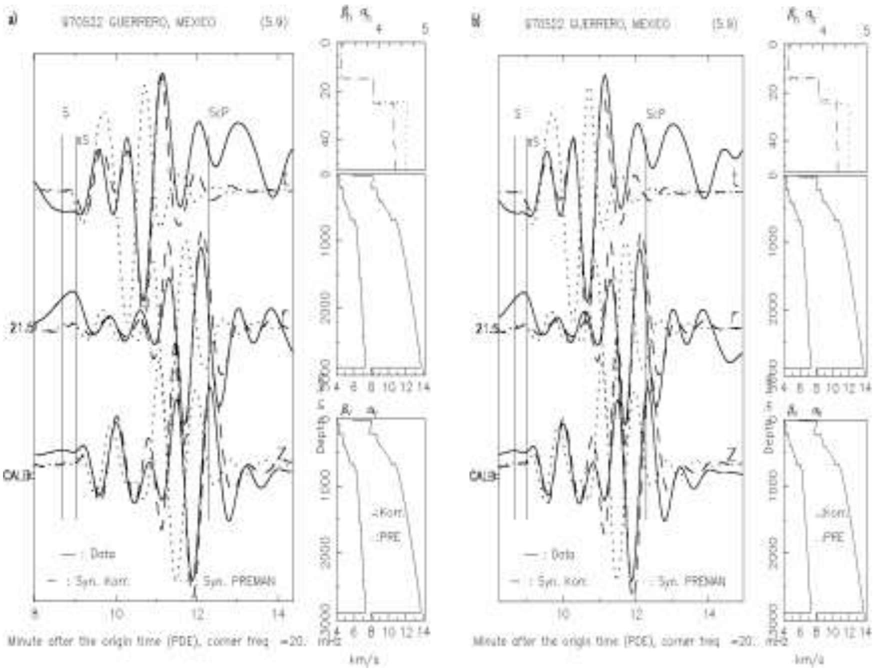

(a) (b)

Figure 5 Seismogram fitting in observation station CALB: a. Analysis using SBC earth model; b. Analysis using CALB earth model.

Next will be shown, how is the seismogram analysis at station CALB, First the obtained earth model between epicenter and station SBC is input for GEMINI program, but then the seismogram analysis is in CALB station carried out. Figure 5a gives illustration for the seismogram comparison. It can be seen, if we pay attention only on the spheroidal components, that waveform fitting is still achieved, where Rayleigh wave in z and r component are nicely fitted, as well as the good fitting of Love surface wave. But synthetic SH wave, neither from SPREM nor from corrected model, arrives later than the real SH wave. Correction is then carried out on the structure of speed β_h on layer below the upper mantle till depth of 771 km. Figure 5b shows the obtained fitting at SH wave. We can see that the arrival time in SH oscillations till Love wave is better simulated, but the synthetic amplitude height is lower than the SH real waveform. The difference on β_h speed structure below the upper mantle between this two observation stations, SBC And CALB show the indication that anisotropy and heterogeneity are not only occurred in upper mantle but on deeper layers till depth of 771 km.

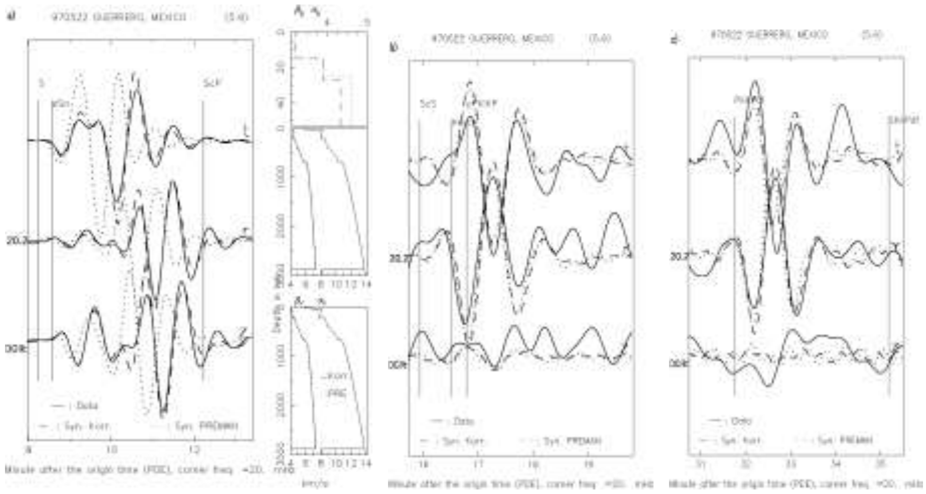

(a) (b) (c)

Figure 6 Seismogram fitting in observation station DGR, time windows of: (a) S, Love and Rayleigh wave; (b) ScS wave; (c) ScS_2 wave.

Figure 6 presents seismogram analysis on various wave phases in DGR observation station. The earth model from each couple epicenter -- observation station is unique; it differs from earth model for the station of SBC and CALB. Figure 6a shows very well fitting for time window from S wave till Rayleigh wave. It can be seen that the bending of waveform curve in time of 9'28" is better simulated, where this is not reached by the synthetic seismogram from SPREM model. In the spheroidal components in the time window from the SV wave till the Rayleigh wave is also better fitted by corrected seismogram. Figures 6b and 6c show seismogram comparison for the wave phase ScS and ScS_2 in DGR observation. The earth model obtained for the fitting of Love and Rayleigh wave and S wave, where the correction is by gradient change in upper mantle and zero order coefficients of speed function in each layer till depth of 771 km achieved. To complete the fitting on these depth phases is a small change values in the speed function for the layers in base mantle also carried out. The waveform fitting is for these depth phases then achieved, which the method of waveform comparison in domain time has the excellence advantage than method of differential travel time [23].

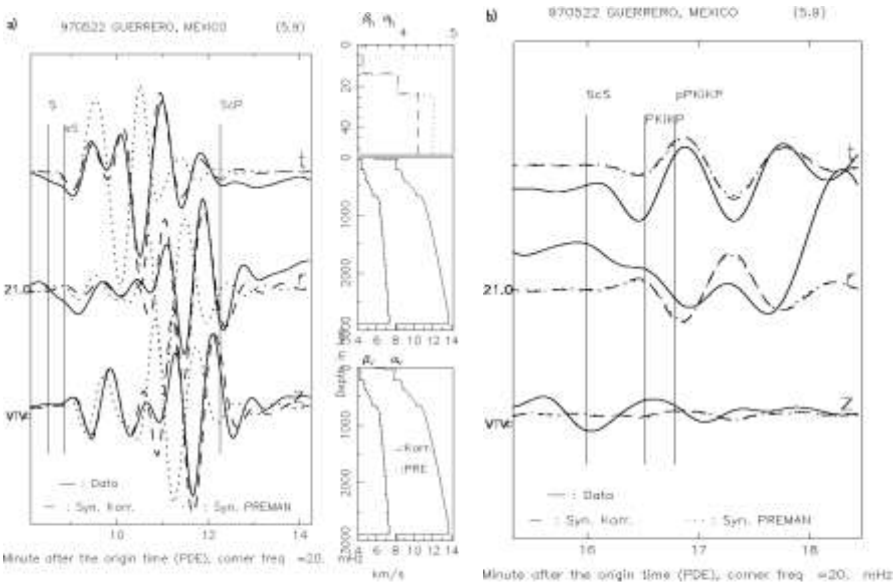

(a) (b)

Figure 7 Seismogram fitting in observation station VTV, times windows for a. S, Love and Rayleigh wave; b. ScS wave.

Hereinafter we analyze the seismogram recorded by observation station VTV for some time windows that is S wave, Love and Rayleigh wave and ScS wave as illustrated in Figure 7. Figure 7a shows seismogram fitting for a time window from S wave till Rayleigh wave. It can be seen, that the SPREM synthetic Love wave has the arrival time, which is earlier than the arrival time of real Love, but the waveform of both seismogram deviates far away. The same phenomena can we also observe that SV wave from SPREM deviates far from the real data. Let we pay attention that resulted fitting between synthetic seismogram from corrected earth model and data seismogram is achieved, that this happened from SH wave till Love wave as well as from SV wave in both z and r components till Rayleigh wave. Figure 7b presents seismogram comparison at ScS wave. It is true that ScS synthetic waveform from SPREM has already the correct arrival time as the real ScS wave. On corrected earth model it is known that the S speed structure on layers till depth of 771 km has to be corrected to obtain the fitting on S wave and surface wave. By so such structure to achieve the fitting on ScS wave the values in layers of mantle base also have to be altered, in such a way till fitting in ScS wave is also obtained.

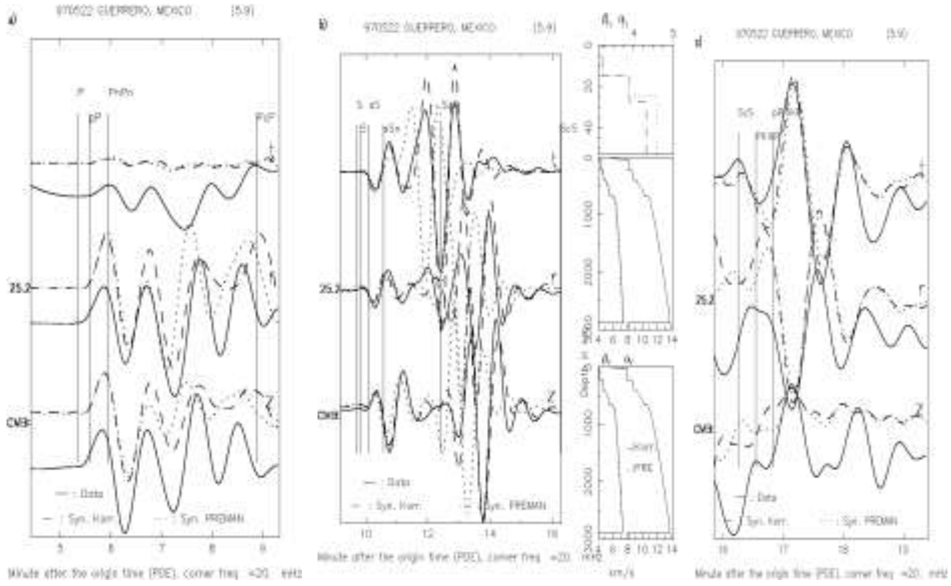

(a) (b) (c)

Figure 8 Seismogram fitting in observation station CMB, time windows for a. P wave; b. S, Love and Rayleigh wave; c. ScS wave

The Figure 8 gives illustration about seismogram comparison in observation station CMB on time windows of P, S, Love and Rayleigh wave and ScS wave. Waveform comparison at phase of S wave let we see in the Figure 8b. Let we pay attention on the S wave at three components simultaneous. SH and SV waves in z component can excellently be simulated by seismogram from corrected earth model, but the fitting on SV wave on r component is not simultaneously achieved. By a vertical anisotropy earth model is the S speed with two parameters presented that are β_h and β_v. These two values are insufficient to explain the deviation that occurred in three S components simultaneously. The synthetic Rayleigh wave from SPREM earth model arrives more early than the real Rayleigh wave, so that correction for the zero order of coefficients has to take a negative value in upper mantle. The Figure 8c shows waveform analysis for ScS wave phase. Correction on speed structure is needed because synthetic ScS wave from earth model SPREM arrives later than the real ScS. Mean a while the observation on S wave shows that the synthetic S wave from SPREM arrives earlier than the real S wave. These two phenomena are contrary, so that the correction value for the layers in upper mantle till depth 771 km takes negative value and for the layers at base mantle takes a positive value. The achieved fitting in ScS wave can we see on this figure. Figure 8a shows waveform comparison on P wave. Let us see that the correction on S speed structure brings repair for the P wave.

The Figure 9 presents seismogram comparison in observation station SNCC. At minute 9'40" let we pay attention that the synthetic waveform from SPREM in t component has shown a weak/flat waveform bending, as the waveform moves from S wave to Love wave. The corrected waveform simulates this bending excellently, as illustrated in Figure 9. The entire waveform from S wave till Love wave on t component can be better simulated. Meanwhile at z component we can see, that the real waveform, from S wave till the end of Rayleigh wave, can theirs arrival times better be simulated by the corrected seismogram, but not the amplitude height. The wave can be analyzed only till the surface wave, because the data quality in later time window is low.

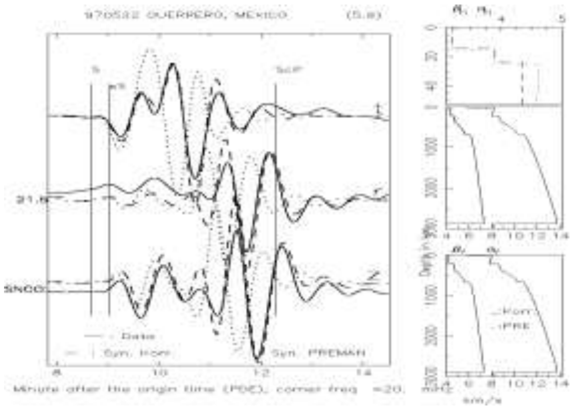

Figure 9 Seismogram fitting in observation station SNCC, time window for S wave, Love and Rayleigh wave.

The Figure 10 shows seismogram analysis and fitting in observation station HKT. The epicentral distant this station is 12.4^0, short enough that there is a big possibility to see the clear ScS wave phase. We start first with the analysis on P wave (the Figure 10a). It can be seen that the good fitting of P wave in r component is achieved, but at z component the synthetic P arrives little later than the real P. This is the contribution from structure of S speed S at fitting of P wave. To repair the delay in z component of the P wave furthermore, we need that the earth model should with an anisotropy model.

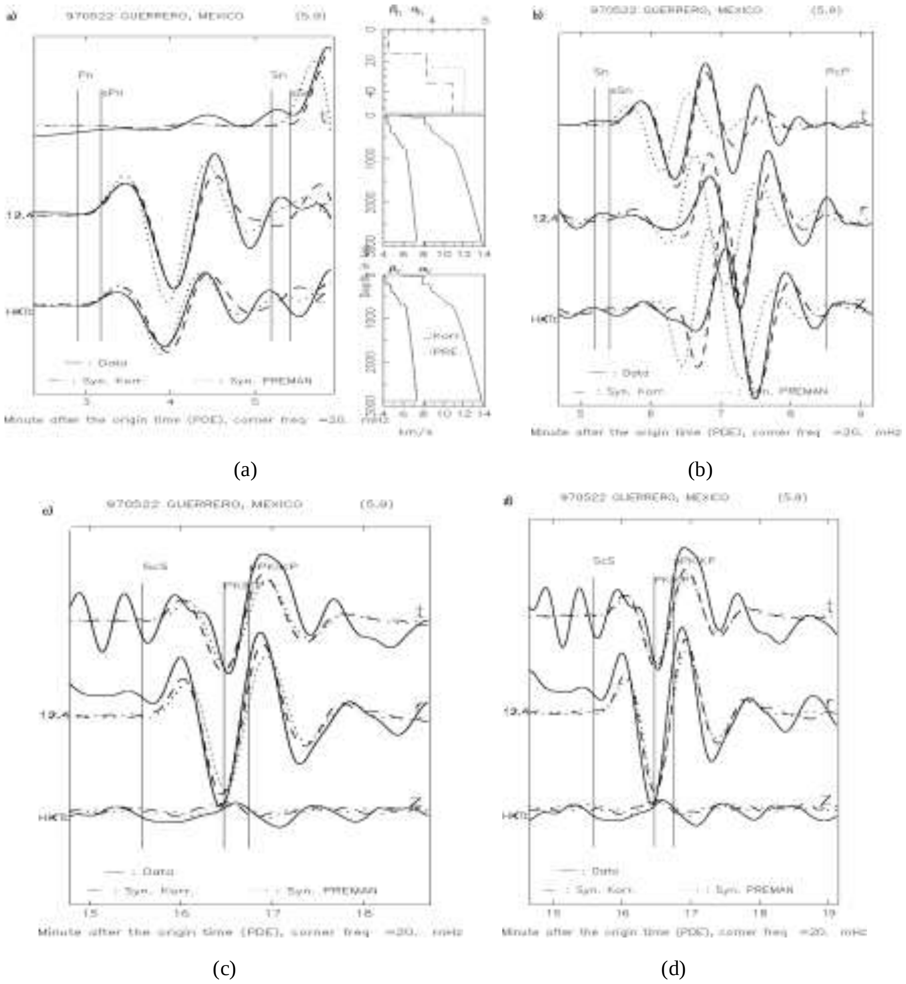

(a) (b)

(c) (d)

Figure 10 Seismogram fitting in observation station HKT, time windows a. P wave; b. S, Love and Rayleigh wave; c. ScS-r wave; d. ScS-t wave.

The Figure 10b shows seismogram analysis and fitting in time window of S wave, Love and Rayleigh surface wave. It can be seen that good waveform fitting can only be reached from S wave till the main maximum of the Love wave, but the end oscillation of the Love wave cannot be achieved. Good fitting on main oscillation of Love wave is reached by change of earth crust thickness (Moho Depth), but remain cannot repair the amplitude height on end oscillation of Love wave. At the fitting of Rayleigh wave let we pay attention that the Rayleigh wave does not react significantly to the change of Moho depth. The Figure 10c shows seismogram fitting that occurred on ScS wave in r component. To achieve the fitting on the S mantle wave, the S-wave velocity structure in the upper 639 km has corrected. But this correction doesn't bring any repair on the ScS wave phase. So that the fitting is continued by the change of S speed on β_v component in the base mantle, so that this fitting is achievable. At this picture can we also see that synthetic wave ScS in t component t arrives earlier than real ScS. The Figure 10d shows the correct arrival time of synthetic wave ScS in t component. This fitting is obtained by altering the value of β_v. If the value of β_v as for Figure 10c is defended, change at β_h in the base mantle does not bring the influence at fitting of ScS wave in t component. The difference of β_v and β_h values in the base mantle shows that the anisotropy is also occurred in the base mantle. This is the question for the speed model of β in the base mantle.

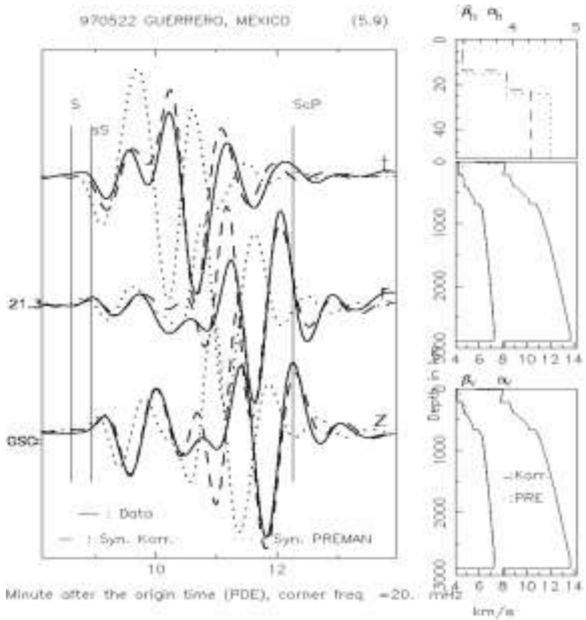

Figure 11 Seismogram fitting in observational station GSC, time window of S, Love and Rayleigh wave.

The Figure 11 presents seismogram analysis and fitting in station GSC. It can be seen in minute of 9'55" that the synthetic waveform from SPREM has no small bending, while synthetic waveform from corrected gives the bending as good as the real waveform. At z and r components we see the good fitting at both SV wave. The fitting on both kind of surface wave Love and Rayleigh can better be achieved by synthetic waveform from corrected model.

From the series of Figures 4 – 11 above we have seen how far the deviation is by seismogram comparison between data and the synthetics one from standard earth model, if the analysis is carried out in time domain and three Cartesian components simultaneously. Although corner frequency of a low pass filter is set at 20 mHz, in the reality the waveform comparison give indication that the waveform is very sensitive to earth model. The obtained correction to the 1-D earth model in every couple of epicenter – observation station is unique. To obtain the S speed structure is waveform analysis in time domain gives better method than by noting the arrival time of S wave, which the measurement is not so easy due lower frequency and in the noisy time series. The method of dispersion analysis measures the indirect data from seismogram that is dispersion curves for the phase/group velocity to frequency. These kinds of data were intensive usable by seismology to determine the earth model.

Table 1 shows the zero order coefficients of SV and SH velocity functions from two stations, SBC and DGR. If we compare the values of SV and SH in earth radius from 3480 km (Core Mantle Boundary, CMB) to 6291 km, these two stations have different values for the same earth layer. The same values are occurred only on the lower and upper crust, but the thickness of earth crust below these stations is different.

Table 1 Zero order coefficients of SV and SH wave velocity of SBC and DGR stations.

SBC			***DGR***		
R	***SV***	***SH***	***R***	***SV***	***SH***
3480.0	6.9354	6.9254	3480.0	6.9654	6.9754
3630.0	11.1871	11.1771	3630.0	11.2071	11.1971
5600.0	22.3659	22.3559	5600.0	22.3859	22.3959
5701.0	9.9939	9.9939	5701.0	10.0039	10.0039
5771.0	22.3512	22.3512	5771.0	22.3512	22.3712
5971.0	8.9496	8.9496	5971.0	8.9496	8.9696
6151.0	5.6323	5.7632	6151.0	5.6283	5.7502
6291.0	5.6323	5.7632	6291.0	5.6283	5.7502
6346.0	4.0000	4.0000	6343.6	4.0000	3.9000
6356.1	3.3000	3.2000	6356.0	3.3000	3.2000

The 6 stations are located quite closely together and the data should reflect the differently deep Earth structure. Any difference in the earth crust below the stations are be due to very local differences in the site condition

4 Conclusion

Seismogram data from earthquake C052297B, Guerrero, Mexico has been analyzed. The seismogram comparison is executed in time domain and three components simultaneously, different with other seismological data; travel time and dispersion data. Both seismograms were a low-pass filter with corner frequency at 20 mHz imposed. In this research the two standard earth models are tested through the seismogram comparison using GEMINI program that is a program to calculate complete synthetic seismogram. There is unsystematic deviation between real and the synthetics waveform from both model of standard earth at various phases of surface wave, body waves and depth wave.

To accomplish the deviation, S speed model in upper mantle is altered to positive gradient for S speed and changes in values of zero order coefficients for the β_v and β_h in the upper mantle and change in earth crust thickness. This brings good fitting to surface wave of Love and Rayleigh simultaneously. To accomplish the deviation of body wave, the speed model at layers below till depth of 771 km is altered in such a way till the fitting at waveform of S wave is achieved. To obtain the fitting at depth waves like ScS and ScS_2 the speed change is till layers in base mantle executed. This method gives new way to investigate the S speed structure near CMB using station with small epicentral distance. In some station, change of S speed structure S gives the contribution to the solving of deviation at P wave. The earth model in this area has strong negative anomalies on S wave velocity. Earth models obtained to every couple of station – observation station has unique character, from earth crust thickness, upper mantle, layers till depth 771 km and layers in the base mantle. This shows the heterogeneity and anisotropy of the earth model beneath Southwest of North America landmass.

Acknowledgement

Gratitude is addressed to Dr. Dalkomo and Prof. Friedrich that has developed the GEMINI program with me, as well as to Prof. Wielandt. Gratitude is also addressed to IRIS (International Seismogram Network) that has provided the seismogram data for this research and its complementary software. The main program was written with the non-commercial software Intel FORTRAN, and the pictures in this paper are written with the PGPLOT and GMT software.

Reference

[1] Dziewonski, A.M. & Anderson, D.L., *Preliminary Reference Earth Model*, Phys. of the Earth and Plan. Int., **25**, 297-356, 1981.
[2] Kennett, B.L.N., IASPEI91 1991, Seismological Tables, Research School of Earths Sciences, Australian National University, 1991.
[3] Kennett, B.L.N., Engdahl, E.R. & Buland, R., *Constraints on Seismic Velocities in the Earth from Travel Times*, Geophys. J. Int., **122**, 108-124, 1995.
[4] Gubbins, D., *Seismology and Plate Tectonics*, Cambridge University Press, Cambridge, 1990.
[5] Keyser, M., Ritter, J. & Jordan, M., 3*D Shear-Wave Velocity Structure of the Eifel Plume*, Germany, Earth and Plan. Sci. Letters, **203**, 59-82, 2002.
[6] Tanaka, S., *Very Low Shear Wave Velocity at the Base of the Mantle under the South Pacific Superswell*, Earth and Plan. Sci. Letters, **203**, 879-893, 2002.
[7] Frederiksen, A.W., Bostock, M.G., Van Decar, J.C. & Cassidy, J.F., *Seismic Structure of the Upper Mantle Beneath the Northern Canadian Cordillera from Teleseismic Travel-Time Inversion*, Tectonophysics, **294**, 43-55, 1998.
[8] Souriau, A. & Poupinet, G., *A Study of The Outermost Liquid Core using Differential Travel Times of the SKS, SKKS and S3KS Phases*, Phys. of the Earth and Plan. Int., **68**, Issue 1-2, 183-199, 1991.
[9] Wysession, M.E., Valenzuela, R.W., Zhu, A. & Bartkö, L., *Investigating the Base of the Mantle using Differential Travel Times*, Phys. of the Earth and Plan. Int., **92**, Issue 1-2, 67-84, 1995.
[10] Dziewonski, A., Block, S. & Landisman, M., *A Technique for The Analysis of Transient Seismic Signals*, Bulletin of the Seismological Society America, **59**, 427-444, 1969.
[11] Herrin, E. & Goforth, T., *Phase-Matched Filters: Application to Study of Rayleigh Waves*, Bulletin of the Seismological Society of America, **67**, 1259-1275, 1977.
[12] Feng, M., Assumpcao, M. & van der Lee, R.D., *Group-Velocity Tomography and Lithospheric S-Velocity Structure of the South American Continent*, Phys. of the Earth and Plan. Int., **147**, 315-331, 2004.
[13] van der Lee, R.D., James, A. & Silver, S., *Upper Mantle S-Velocity Structure of Central and Western South America*, J. of Geophys. Res., **106**, No. 12, 30.821-30.885, 2001.
[14] Okabe A., Kaneshima, S., Kanjo, K., Ohtaki, T. & Purwana, *Surface Wave Tomography for Southeastern Asia using IRIS-FARM and JISNET Data*, Phys. of the Earth and Plan. Int., **146**, 101-112, 2003.
[15] Zhao, D., *Global Tomographic Imaging of Mantle Plumes and Subducting Slabs: Insight into Deep Earth Dynamics*, Phys. of the Earth and Plan. Int., **146**, 3-34, 2004.

[16] Kennett, B.L.N., Gudmundsson, O. & Tong, C., *The Upper-Mantle S And P Velocity Structure Beneath Northern Australia From Broad-Band Observations*, Phys. of the Earth and Plan. Int., **86**, 85 – 98, 1994.

[17] Simons, F.J., Zielhuis, A. & van der Hilst, R.D., *The Deep Structure of the Australian Continent from Surface Wave Tomography*, Lithos, **48**, 17-43, 1999.

[18] Debayle, E. & Kennett, B.L.N., *Anisotropy in The Australasian Upper Mantle From Love and Rayleigh Waveform Inversion*, Earth and Plan. Sci. Letters, **184**, 339-351, 2000.

[19] Dalkolmo, J., *Synthetische Seismogramme Fuer Eine Sphaerisch Symmetrische, Nichtrotierende Erde Durch Direkte Berechnung Der Greenschen Funktion*, Diplomarbeit, Inst. fuer Geophys., Uni. Stuttgart, 1993.

[20] Friederich, W. & Dalkolmo, J., *Complete Synthetic Seismograms for a Spherically Symmetric Earth by a Numerical Computation of the Green's Function in the Frequency Domain*, Geophys. J. Int., **122**, 537-550, 1995.

[21] Buland, R. & Chapman, C., *Travel Time Calculation*, Bulletin of the Seismological Society of America, **73**, 1271-1302, 1983.

[22] Friederich, W., *Regionale, dreidimensionale Strukturmodelle des oberen Mantel aus der wellentheoritischen Inversion teleseismischer Oberflaechenwellen*, Berichte des Instituts fuer Geophysik der Universitaet Stuttgart 9, 1997.

[23] Garnero, E.J. & Lay, T., *D'' Shear Velocity Heterogeneity, Anisotropy and Discontinuity Structure Beneath the Caribbean and Central America*, Phys. of the Earth and Plan. Int., 140, 219-242, 2003.